Entropy **2014**, *16*, 2756-2767; doi:10.3390/e16052756

OPEN ACCESS

entropy

ISSN 1099-4300

www.mdpi.com/journal/entropy

Article

Long-Range Atomic Order and Entropy Change at the Martensitic Transformation in a Ni-Mn-In-Co Metamagnetic Shape Memory Alloy

Vicente Sánchez-Alarcos [1], Vicente Recarte [1,*], José Ignacio Pérez-Landazábal [1], Eduard Cesari [2] and José Alberto Rodríguez-Velamazán [3,4]

[1] Departamento de Física, Universidad Pública de Navarra, Campus de Arrosadía, 31006 Pamplona, Spain; E-Mails: vicente.sanchez@unavarra.es (V.S.); ipzlanda@unavarra.es (J.I.P.)

[2] Departament de Física, Universitat de les Illes Balears, Ctra. de Valldemossa, km 7.5, E-07122 Palma de Mallorca, Spain; E-Mail: eduard.cesari@uib.cat

[3] Instituto de Ciencia de Materiales de Aragón, CSIC - Universidad de Zaragoza, 50009 Zaragoza Spain

[4] Institut Laue Langevin, F-38042 Grenoble, France; E-Mail: velamazan@ill.eu

* Author to whom correspondence should be addressed; E-Mail: recarte@unavarra.es; Tel.: +34-948-169-582; Fax: +34-948-169-565.

Received: 4 April 2014; in revised form: 28 April 2014 / Accepted: 14 May 2014 / Published: 19 May 2014

Abstract: The influence of the atomic order on the martensitic transformation entropy change has been studied in a Ni-Mn-In-Co metamagnetic shape memory alloy through the evolution of the transformation temperatures under high-temperature quenching and post-quench annealing thermal treatments. It is confirmed that the entropy change evolves as a consequence of the variations on the degree of $L2_1$ atomic order brought by thermal treatments, though, contrary to what occurs in ternary Ni-Mn-In, post-quench aging appears to be the most effective way to modify the transformation entropy in Ni-Mn-In-Co. It is also shown that any entropy change value between around 40 and 5 J/kgK can be achieved in a controllable way for a single alloy under the appropriate aging treatment, thus bringing out the possibility of properly tune the magnetocaloric effect.

Keywords: Ni-Mn-In-Co; entropy change; atomic order; martensitic transformation; metamagnetic shape memory alloys

---

1. Introduction

Ni-Mn-based Heusler alloys exhibiting both long-range magnetic ordering and thermoelastic martensitic transformation (MT) have been intensively investigated in recent years, from both fundamental and applied points of view, due to the unique properties they show linked to the occurrence of a first-order martensitic transformation (MT) between magnetically ordered phases [1]. The magnetism in these alloys mainly arises from the coupling between the Mn atoms (in which the magnetic moment is chiefly confined), so the magnetic exchange interactions strongly depend on the Mn-Mn distance [2], and therefore different sequences of magnetostructural transformations can be observed depending on both the X element and the change in interatomic distances caused by the MT. In particular, in the so-called metamagnetic shape memory alloys, $Ni_2Mn_{1-x}Z_{1+x}$ (Z=In, Sn, and Sb), the MT takes place between ferromagnetic austenite and a weak magnetic martensitic phase due to weakening of the exchange interactions (competing ferromagnetic and antiferromagnetic) [3–8]. The large change of magnetization, ΔM, occurring at the MT in this case allows the induction of the MT by an applied magnetic field, thus giving rise to multifunctional properties (namely giant magnetoresistance [9–12] magnetic shape memory [13], or large inverse magnetocaloric effect [14,15] of great technical interest for practical applications in sensing and magnetic refrigeration.

The magnetostructural MT in metamagnetic shape memory alloys is mainly driven by lattice dynamics and magnetism. Since the free energy of the ferromagnetic phase depends on the magnetization, a magnetic term appears in the energy balance between austenite and martensite due to the variation of the magnetic exchange coupling at the MT. In this sense, the entropy change linked to the MT can be considered as the sum of a vibrational term and a magnetic term ($\Delta S \approx \Delta S_{vib} + \Delta S_{mag}$) as long as there is no configurational contribution to the entropy change (due to the diffusionless character of the MT) and the electronic contribution is expected to be very small in these alloys [16]. The magnetic contribution, and therefore the entropy change at the MT, can be modified by the application of an external magnetic field [17] and, taking into account that the magnetic moment depends on the configurational ordering of the magnetic atoms in the crystal lattice, by the variation of the long-range atomic order. In this last respect, it has been recently shown that, for a given alloy composition, the atomic order can be easily modified in Ni-Mn-In alloys by means of different thermal treatments [18,19]. In particular, quenching from high temperatures (around the B2-$L2_1$ ordering temperature) allows to partially retain the low atomic order present at these temperatures, in such a way that the degree of long-range atomic order in the as-quenched alloys is lower than the equilibrium value allowed by the stoichiometry, which can be achieved after a slowly enough cooling. Likewise, the metastable state retained after quenching may evolve to the stable state (that is, the equilibrium atomic order degree of the alloy may be restored) once the alloy is heated up to temperatures at with atomic diffusion is possible, as it occurs in Ni-Mn-Ga alloys [20,21]. The increase in atomic order in Ni-Mn-In alloys enhances the magnetic character of the austenite, thus increasing its Curie temperature and lowering the MT temperature. Furthermore, the influence of atomic order on the transformation entropy points out the key role of atomic order on the thermodynamics of the MT in these alloys. In Ni-Mn-Sn and Ni-Mn-Sb, in turn, the $L2_1$ ordering is stable up to very high temperatures and no variation on the atomic order can be brought by thermal treatments [22].

The addition of Cobalt to Ni-Mn-In has been shown to enhance the magnetism of the austenite and to avoid ferromagnetic ordering in martensite [23,24]. This leads to an increase of ΔM at the MT which favors larger magnetically-induced shifts of the transformation temperatures and results in a higher associated magnetocaloric effect [25]. In these quaternary alloys, the entropy change at the transformation, ΔS, strongly varies with the degree of atomic order, which can be tailored by means of the thermal treatment [26]. The observed evolution of ΔS has been correlated to the difference between the Curie and martensitic transformation temperatures, which also depends on composition. However, up to now, no systematic study on the study of the effect of thermal treatments on the transformation entropy in Ni-Mn-In-Co alloys has been performed. In the present work, the influence of the atomic order on the martensitic transformation entropy change has been studied in a Ni-Mn-In-Co metamagnetic shape memory alloy through the evolution of the transformation temperatures under high-temperature quenching and post-quench annealing thermal treatments. It is confirmed that the entropy change evolves as a consequence of the variations on the degree of $L2_1$ atomic order brought by thermal treatments, though, contrary to what occurs in ternary Ni-Mn-In, post-quench aging appears as the most effective way to modify the transformation entropy in Ni-Mn-In-Co. It is also shown that any entropy change value between around 40 and 5 J/kgK can be achieved in a controllable way for a single alloy under the appropriate aging treatment, thus bringing out the possibility of properly tune the magnetocaloric effect.

2. Experimental Section

A polycrystalline $Ni_{45}Mn_{36.7}In_{13.3}Co_5$ (at %) ingot was prepared from high purity elements by arc melting under protective Ar atmosphere. The ingot was remelted several times and then homogenized in vacuum quartz ampoules at 1,173 K during 24 h. Small samples for calorimetric and magnetic measurements were obtained from discs previously cut from the center of the ingots by a slow speed diamond saw, and powder samples for neutron diffraction experiments were elaborated by crushing the samples in an agate mortar. Differential Scanning Calorimetry (DSC) measurements at a heating/cooling rate of 10 K/min were carried out in a TA Q100 DSC to study the thermal behavior of the samples. In order to analyze the effect of high-temperature thermal treatments on the transformation temperatures and the transformation entropy, the alloy was subjected to a 30 minutes annealing treatment at different temperatures (ranging from 773 K to 1173 K) followed by quenching in ice water. On the other hand, thermal cycles through the MT after heating up to different temperatures were performed on the as-quenched samples in order to observe "in situ" the evolution of the Curie and MT temperatures with the post-quench thermal treatments. The atomic order was analyzed by neutron diffraction measurements carried out at the Institute Laue-Langevin (Grenoble, France). In particular, powder neutron diffraction measurements were performed at a wavelength of 1.28 Å.

3. Results and Discussion

Figure 1 shows the DSC thermograms obtained on a cooling-heating ramp in the vicinity of the martensitic transformation of the as-quenched samples. As indicated, the exothermic and endothermic peaks correspond to the forward and reverse martensitic transformations, respectively, and the λ-type shoulders are associated to the magnetic ordering of the austenite at the Curie temperature, T_C. In order

to track the evolution of the MT, the temperatures of the MT peaks maxima, T_m^{for} and T_m^{rev}, have been taken as the forward and reverse MT temperature, respectively.

Figure 1. DSC thermograms corresponding to quenching from different temperatures.

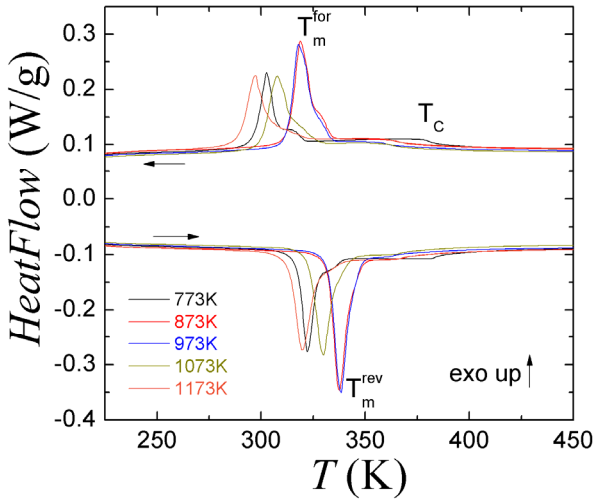

As shown in Figure 2a, both the MT and Curie temperatures evolve with the quenching temperature, T_{quench}, though showing a non-monotonous behavior. In particular, the MT temperature T_m increases and T_C decreases with the increasing T_{quench} for T_{quench} < 900 K, and the opposite behavior, that is, a decrease on T_m and a slight increase on T_C, is observed when quenching from above 900K. The evolution of the transformation temperatures for T_{quench} < 900 K is similar to that found in ternary Ni-Mn-In, and can be ascribed to a decrease of the retained degree of $L2_1$ atomic order on increasing the quenching temperature [19]. On the other hand, assuming that quenching mainly affects the transformation temperatures due to the modification of atomic order, the behavior of T_m and T_C for T_{quench} > 900 K could be related to an increase of the retained degree of atomic order with the increasing T_{quench}, promoted by a high vacancies concentration at the quenching temperature that assist the ordering process, as in fact occurs in Ni-Mn-Ga and Ni-Fe-Ga alloys [20,27]. In any case, the net variations of the MT temperature ($\Delta T_m \approx 20$ K) are much lower than those found in Ni-Mn-In subjected to exactly the same quenching treatments ($\Delta T_m > 60$ K) [19], thus pointing out either a lower effect of quenching on the retained atomic order or a lower influence of atomic order on the MT. From the latent heat estimated from the area bellow the peaks in Figure 1, Q, the corresponding entropy change at the MT has been calculated as $\Delta S = Q/T_m$. The absolute values of the entropy change at the forward and reverse MT (ΔS_{for} and ΔS_{rev}, respectively) are plotted as a function of T_{quench} in Figure 2b. Although the absolutes values of ΔS_{for} and ΔS_{rev} are slightly different (as a result of the combination of the strong dependence of the magnetic contribution ΔS_{mag} on the temperature and the hysteresis of transformation) the evolution is almost the same in both cases; ΔS increases with T_{quench} for T_{quench} < 900 K and slightly decreases with T_{quench} for T_{quench} > 900 K. From the values in Figure 2a, it can be seen that the higher is the difference T_C-T_m the lower the entropy change, in agreement with previous results on similar alloys [26]. In this sense, the lower net variations of ΔS under quenching comparing with ternary Ni-Mn-In ($\Delta (\Delta S_{NiMnInCo}) \approx 10$ *J/kgK* vss $\Delta (\Delta S_{NiMnIn}) \approx 16$ *J/kgK*) can be understood as a direct consequence of the smaller effect of quenching on the transformation temperatures.

Figure 2. Transformation temperatures (**a**) and absolute value of the entropy change at the MT (**b**) as a function of the quenching temperature.

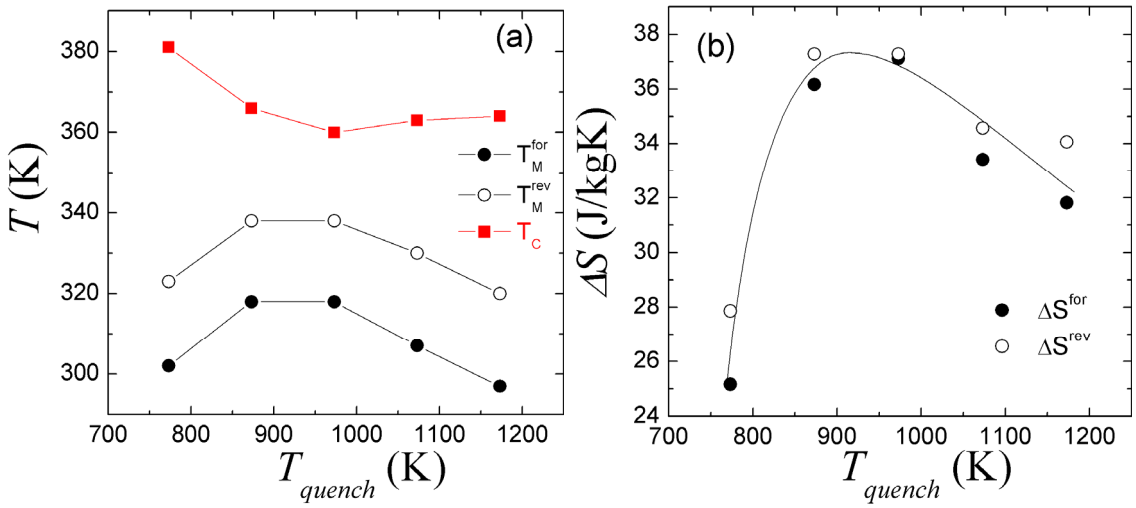

In order to analyze the effect of thermal treatments on the atomic order, the temperature dependence of long range atomic order has been evaluated from neutron powder diffraction measurements. Figure 3a shows the neutron diffractogram obtained at 400 K (in paramagnetic austenite, to avoid magnetic contributions) on a powder sample quenched from 723 K. The alloy displays the cubic $L2_1$ structure typical of Heusler compounds, with lattice parameter a=5.9692 *Å*. The intensity peaks have been indexed according to the associated Bragg reflections.

Figure 3. (**a**) Neutron diffractogram obtained at 400 K on a powder sample quenched from 723 K. (**b**) Temperature dependence of the $L2_1$ order parameter.

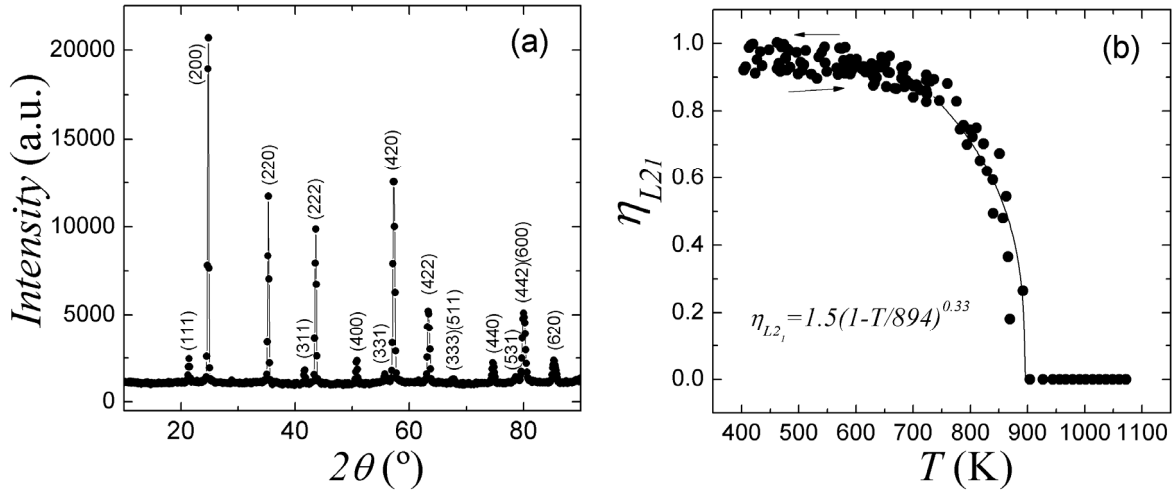

The evolution of the $L2_1$ atomic order with temperature has been estimated from the evolution of the integrated intensity of the austenitic (111) reflections, which are exclusively linked to that type of ordering (according to the corresponding unit cell structure factor, the $L2_1$ superstructure reflections are those in which the h, k, l indices are all odd). In particular, the order parameter corresponding to the $L2_1$ structure, η_{L21} (which ranges from 0, for the B2 structure, to 1, for the maximum next-nearest-neighbor atomic order allowed by the stoichiometry), has been determined assuming

$\eta_{L21} \sim I_{111}^{1/2}$ and normalizing to the I_{111} value measured at 400 K after slowly cooling from 1,170 K [28]. Figure 3b shows the temperature dependence of the $L2_1$ order parameter on heating-cooling between 400 K and 1,173 K. The degree of $L2_1$ atomic order progressively decreases on heating above 700 K, until it becomes zero (the intensity of the (111) reflection completely vanishes) at around 900 K, thus evidencing the occurrence of a $L2_1 \leftrightarrow B2$ ordering transition. Since this transition has a second-order character, the behavior of η_{L21} when approaching the transition has been fitted to the power law $\eta_{L21} = A\ (1-T/T_{ord})^{\beta}$, obtaining values of $T_{ord} = 894\ K$, $A = 1.5$ and $\beta = 0.33$. The values of A and β parameters are consistent with the theoretical ones for a three-dimensional Ising model [29], and the value of the transition temperature T_{ord} is similar to that observed in the corresponding ternary $Ni_{50}Mn_{37}In_{13}$ alloy [30]. The degree of atomic order is close to unity below 750 K and becomes irrelevant above 900 K. Besides, a good agreement between heating and cooling curves is observed. Then, the quenching temperatures where substantial differences could be expected correspond to the 750–900 K temperature range. On the other side, the vacancies concentration at the different temperatures and their evolution must also play an important role during the quenching process and on the final order degree obtained at room temperature. So, the low influence of quenching on the transformation temperatures and on the MT entropy change can be explained since the atomic disorder retained by quenching is almost the same in all samples (except at 753 K where a large order degree is obtained).

Nevertheless, the atomic order can be better correlated with T_m, T_C and ΔS by means of post-quenched thermal treatments, taking into account that the equilibrium atomic order degree of the alloy may be restored once the alloy is heated up to a temperatures where atomic diffusion is possible. As previously reported in Ni-Mn-Ga and Ni-Mn-In alloys, the metastable-to-stable post-quench ordering process gives rise to an exothermic peak on the first heating curve of the DSC thermograms which makes it possible to identify and analyze the ordering process from calorimetric measurements. The exothermic peak associated with the post-quench ordering process taking place in the sample quenched from 1,073 K can be seen in the thermogram shown in Figure 4a. The inset shows a detail of the exothermic peaks appearing for different quenching temperatures. In order to determine the effect of the post-quench ordering process on the transformation temperatures and the entropy change, several consecutive heating/cooling DSC thermal cycles have been performed on the as-quenched samples. The cycles have been carried out at 10 K/min from a temperature below the MT to a temperature higher in each new cycle, in such a way that each cycle can be considered as a new aging treatment. As shown in Figure 4b, this procedure makes it possible to observe "in situ" the evolution of T_m and T_C as a consequence of the partial development of the ordering process.

Figure 5a shows the increment on T_m^{rev} and T_C as a function of post-quench aging temperature, T_{aging} (that is, the maximum temperature of the DSC partial cycles). The DSC exothermic peak associated with the ordering process is also plotted in the figure. T_m^{rev} highly decreases ($\Delta T_m^{rev} \approx 70\ K$) whereas T_C increases ($\Delta T_C \approx 30\ K$) with the increasing T_{aging}, concurrently with the occurrence of the exothermic peak. This behavior is very similar to that observed in ternary Ni-Mn-In subjected to exactly the same thermal treatments, though the shifts are considerably lower in this latter case, $\Delta T_m^{rev} \approx 30\ K$ and $\Delta T_C \approx 15\ K$, and it is in agreement with previous results on the effect of atomic order on the MT temperature in Co-doped Ni-Mn-In alloys [26]. The increase of the austenite Curie temperature as a result of the atomic ordering process is common to Ni-Mn-Ga and Ni-Mn-In alloys, and it origin relies on the enhancement of the ferromagnetic coupling between Mn atoms as the structure is getting

ordered. Likewise, as it has been recently proposed, the enhancement of ferromagnetic coupling brought by the atomic ordering stabilizes the structural phase showing higher magnetic moment (in this case, the ferromagnetic austenite against the paramagnetic martensite) thus giving rise to a decrease of the MT temperature [31]. In this sense, the higher influence of post-quench aging on T_m and T_C observed in Ni-Mn-In-Co (with respect to the ternary alloy [19]) may be a consequence of both a higher retained atomic disorder, which would be in agreement with its lower T_{ord}, and the higher saturation magnetization of the quaternary austenite. In any case, it is worth noting that the post-quench atomic ordering process results in a larger increase of the T_C-T_m difference, which leads to a considerably higher decrease of the entropy change at the MT ($\Delta(\Delta S_{NiMnInCo}) \approx 25$ *J/kgK vs* $\Delta(\Delta S_{NiMnIn}) \approx 7$ *J/kgK*), as shown in Figure 5b, where the increment of the entropy change at the MT with respect to the as-quenched state, $\Delta(\Delta S)$, is shown as a function of the post-quench aging temperature (for the sake of clarity, just the reverse MT is shown). With respect to the effect of atomic ordering on the transformation entropy ΔS, two main contributions, $\Delta S \approx \Delta S_{vib} + \Delta S_{mag}$, where ΔS_{vib} is the vibrational contribution and ΔS_{mag} is the magnetic contribution, can be considered (as already said, the electronic contribution ΔS_{el} is expected to be very small, even more if the alloy composition is not modified). In the case of the reverse MT, both terms in the entropy balance have opposite signs; $\Delta S_{vib} > 0$ due to the excess of vibrational entropy of the austenite with respect to the martensite [32], and $\Delta S_{mag} < 0$ as result of a MT from a magnetically disordered phase to an ordered one. Since the austenitic and martensitic overall structures do not evolve with atomic ordering, a similar variation on the density of vibrational states is expected in both phases, and consequently the effect of atomic ordering on ΔS_{vib} can be neglected in a first approximation, so the influence of atomic order on ΔS must be linked just to the change of ΔS_{mag} as a consequence of the variations in the magnetic exchange coupling in the austenitic phase.

Figure 4. (**a**) DSC thermograms obtained on heating the sample just quenched from 1,073 K. Inset: detail of the exothermic peak associated to the ordering process in the samples quenched from different temperatures. (**b**) DSC thermograms performed on several consecutive thermal cycles on the sample just quenched from 1,073 K.

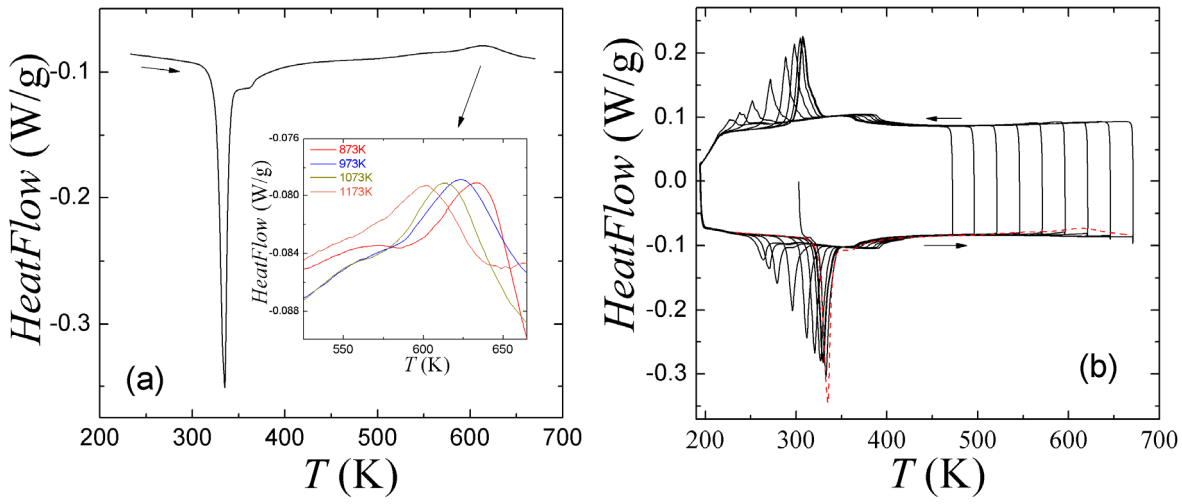

Figure 5. Increment on T_m^{rev} and T_C (**a**) and increment on the transformation entropy at the reverse MT (**b**) in the sample quenched from 1,070K, as a function of post-quench aging temperature. Inset: Increment on the transformation entropy in Ni-Mn-In [19].

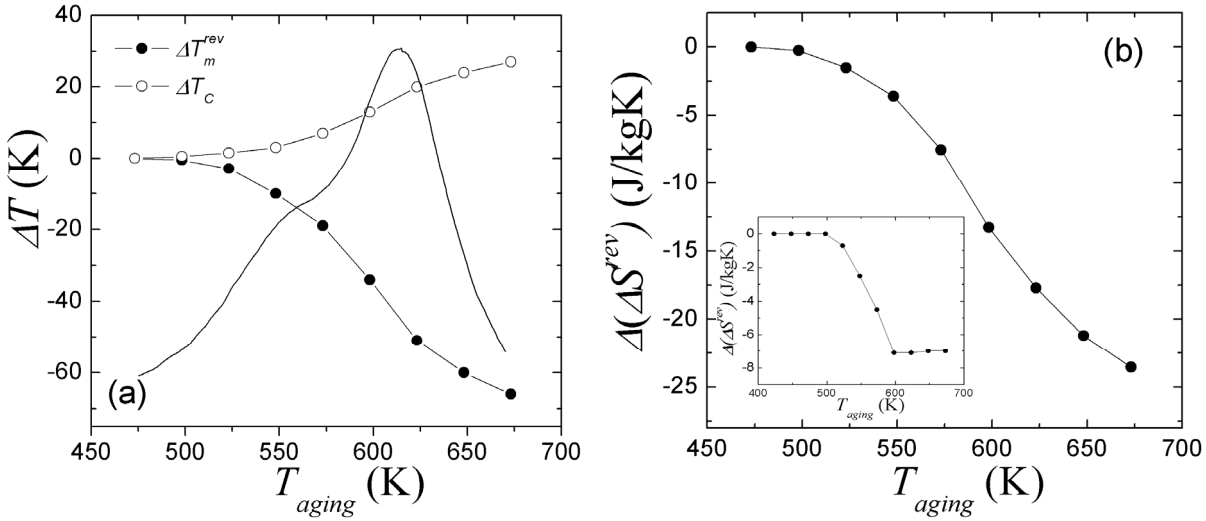

Figure 6. Increment on T_m and T_C (**a**), and increment on the absolute value of the transformation entropy (**b**), in the samples quenched from different temperatures and followed by cyclic post-quench ageing (for T_m and ΔS. closed symbols: direct MT; open symbols: reverse MT).

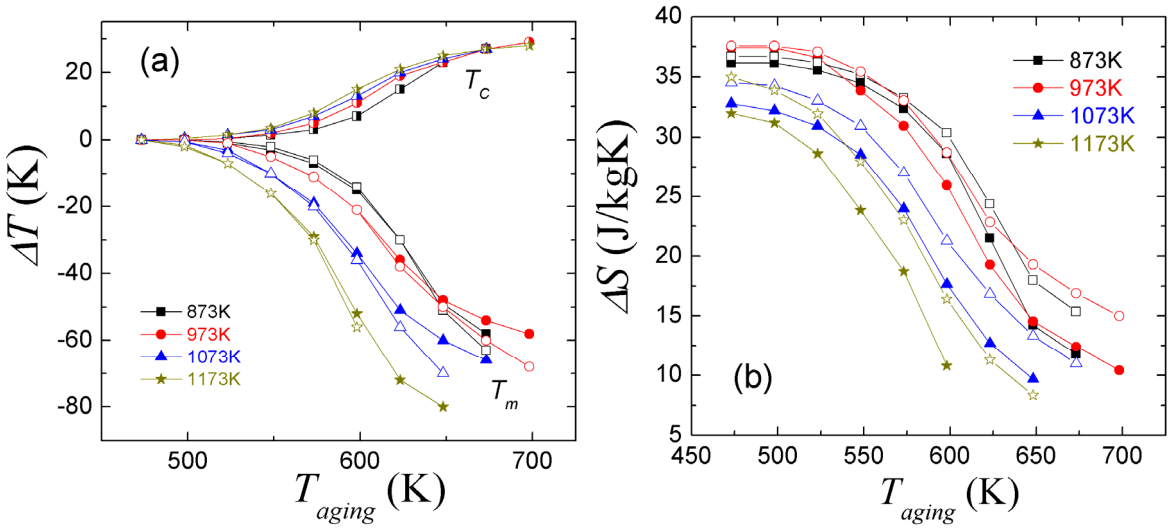

The comparison between Figure 2b and Figure 5b confirms that post-quench aging is more effective than high temperature quenching to control the entropy change through atomic order variations, contrary to what occurs in the corresponding ternary Ni-Mn-In [18,19]. This is quite interesting since it means that almost any ΔS value between around *40 J/kgK* and *5 J/kgK* can be achieved in a controllable way for a single alloy. In fact, taking into account that the limit value of the magnetocaloric effect is the transformation entropy (if the effect of the magnetic field is strong enough to totally induce the first order transition) [33], this brings out the possibility of properly tune the magnetocaloric effect, which can be tailored in a continuous way by choosing the appropriate aging temperature. Furthermore, the range of achievable entropy values can be broadened by quenching the

alloy from different temperatures. In this respect, Figure 6 shows the increments on T_m and T_C (Figure 6a) and the corresponding absolute values of the entropy change achievable at forward and reverse MT (Figure 6b) for the alloy quenched from 873 K, 973 K, 1,073 K and 1,173 K (from which a similar degree of atomic order is retained) and followed by cyclic post-quench ageing. It can be seen that, in fact, a very large range of entropy change values are obtained for a single alloy from the combination of quenching and post-quench treatments. As stated above, the evolution of the transformation entropy under thermal treatments is caused by the evolution of the magnetic contribution ΔS_{mag} as a consequence of the effect of long-range atomic order on the alloy magnetism.

The role of the magnetic contribution to the transformation entropy becomes evident from the common dependence of the measured ΔS values on the normalized temperature difference, $\delta_A = (T_C - T_m)/T_C$, shown in Figure 7. This behavior agrees with the phenomenological model based on a Bragg-Williams approximation recently proposed to describe the evolution of the magnetic contribution to the total entropy change in Ni-Mn-based alloys [34] (a similar behavior has been also reported in Ni-Fe-Ga ferromagnetic shape memory alloys [35]). The absence of a marked change in the slope (previously reported) seems to be due to the paramagnetic nature of martensite in the present Ni-Mn-In-Co alloy. Furthermore, the huge set of values presented in the figure perfectly illustrates the above-mentioned ability of thermal treatments to modify the entropy change at MT as a result of the atomic order variations.

Figure 7. Dependence of the measured entropy change values on the normalized temperature difference, $\delta_A = (T_C - T_m)/T_C$.

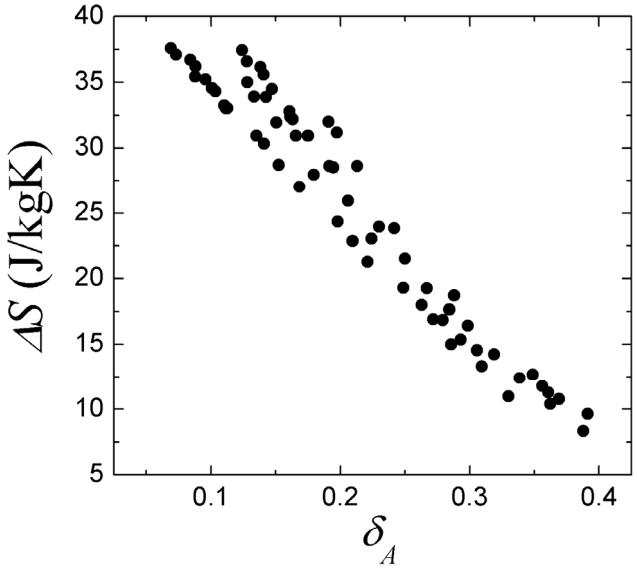

4. Conclusions

The influence of the atomic order on the martensitic transformation entropy change has been studied in a Ni-Mn-In-Co metamagnetic shape memory alloy. The entropy change evolves as a consequence of the variations on the degree of $L2_1$ atomic order brought by thermal treatments. In particular, the evolution of ΔS is explained in terms of the variation of the magnetic contribution to the entropy as a consequence of the change in the magnetic exchange coupling in the austenitic phase.

Contrary to what occurs in ternary Ni-Mn-In, post-quench aging appears as the most effective way to modify the transformation entropy in Ni-Mn-In-Co. Almost any entropy change value between around 40 and 5 J/kgK can be achieved in a controllable way for a single alloy under the appropriate aging treatment, thus bringing out the possibility of properly tune the magnetocaloric effect.

Acknowledgments

This work has been carried out with the financial support of the Spanish "Ministerio de Economía y Competitividad" (projects number MAT2011-28217 C02-01 and MAT2012-37923 C02-01). The Institute Laue Langevin-Spanish CRG D1B installation is acknowledged for the allocated neutron beamtime (Exp. CRG 1905).

Author Contributions

Vicente Sánchez-Alarcos, Vicente Recarte, José Ignacio Pérez-Landazábal and Eduard Cesari wrote the manuscript. Eduard Cesari synthesized the samples. José Alberto Rodríguez-Velamazán performed temperature dependent neutrons diffraction experiments. Vicente Sánchez-Alarcos, Vicente Recarte, José Ignacio Pérez-Landazábal performed calorimetric measurements. All authors have read and approved the final manuscript.

Conflicts of Interest

The authors declare no conflict of interest.

References and Notes

1. Kainuma, R.; Ito, W.; Umetsu, R.Y.; Khovaylo, V.V.; Kanomata, T. Metamagnetic shape memory effect and magnetic properties of Ni-Mn based Heusler alloys. *Mater. Sci. Forum* **2011**, *684*, 139–150.
2. Sasioglu, E.; Sandratskii, L.M.; Bruno, P. First-principles calculation of the intersublattice exchange interactions and Curie temperatures of the full Heusler alloys Ni_2MnX (X = Ga,In,Sn,Sb). *Phys. Rev. B* **2004**, *70*, 024427.
3. Sutou, Y.; Imano, Y.; Koeda, N.; Omori, T.; Kainuma, R.; Ishida, K.; Oikawa, K. Magnetic and martensitic transformations of NiMnX (X = In,Sn,Sb) ferromagnetic shape memory alloy. *Appl. Phys. Lett.* **2004**, *85*, 4358–4360.
4. Krenke, T.; Acet, M.; Wassermann, E.F.; Moya, X.; Mañosa, L.; Planes, A. Martensitic transitions and the nature of ferromagnetism in the austenitic and martensitic states of Ni-Mn-Sn alloys. *Phys. Rev. B* **2005**, *72*, 014412.
5. Oikawa, K.; Ito, W.; Imano, Y.; Sutou, Y.; Kainuma, R.; Ishida, K.; Okamoto, S.; Kitakami, O.; Kanomata, T. Effect of magnetic field on martensitic transition of $Ni_{46}Mn_{41}In_{13}$ Heusler alloy. *Appl. Phys. Lett.* **2006**, *88*, 122507.
6. Krenke, T.; Acet, M.; Wassermann, E.F.; Moya, X.; Mañosa, L.; Planes, A. Ferromagnetism in the austenitic and martensitic states of Ni-Mn-In alloys. *Phys. Rev. B* **2006**, *73*, 174413.

7. Khan, M.; Dubenko, I.; Stadler, S.; Ali, N. Exchange bias behavior in Ni-Mn-Sb Heusler alloys. *Appl. Phys. Lett.* **2007**, *91*, 072510.
8. Aksoy, S.; Acet, M.; Deen, P.P.; Mañosa, L.; Planes, A. Magnetic correlations in martensitic Ni-Mn-based Heusler shape-memory alloys: Neutron polarization analysis. *Phys. Rev. B* **2009**, *79*, 212401.
9. Yu, S.Y.; Liu, Z.H.; Liu G.D.; Chen, J.L.; Cao, Z.X.; Gu, G.H.; Zhang, B.; Zhang, X.X. Large magnetoresistance in single-crystalline $Ni_{50}Mn_{50-x}In_x$ (x = 14–16) upon martensitic transformation. *Appl. Phys. Lett.* **2006**, *89*, 162503.
10. Sharma, V.K.; Chattopadhyay, M.K.; Shaeb, K.H.B.; Chouhan, A.; Roy S.B. Large magnetoresistance in $Ni_{50}Mn_{34}In_{16}$ alloy. *Appl. Phys. Lett.* **2006**, *89*, 222509.
11. Wang, B.M.; Liu, Y.; Wang, L.; Huang, S.L.; Zhao, Y.; Yang, Y.; Zhang, H. Exchange bias and its training effect in the martensitic state of bulk polycrystalline $Ni_{49.5}Mn_{34.5}In_{16}$. *J. Appl. Phys.* **2008**, *104*, 043916.
12. Pathak, A.K.; Gautam, B.R.; Dubenko, I.; Stadler, S.; Ali, N. Phase transitions and magnetoresistance in $Ni_{50}Mn_{50-x}In_x$ Heusler alloys. *J. Appl. Phys.* **2008**, *103*, 07F315–07F315.
13. Du, J.; Zheng, Q.; Ren, W.J.; Feng, W.J.; Liu, X.J.; Zhang, Z.D. Magnetocaloric effect and magnetic-field-induced shape recovery effect at room temperature in ferromagnetic Heusler alloy Ni-Mn-Sb. *J. Phys. Appl. Phys.* **2007**, *40*, 5523.
14. Krenke, T.; Duman, E.; Acet, M.; Wassermann, E.F.; Moya, X.; Mañosa, L.; Planes, A. Inverse magnetocaloric effect in ferromagnetic Ni-Mn-Sn alloys. *Nat. Mater.* **2005**, *4*, 450–454.
15. Planes, A.; Mañosa, L.; Acet, M. Magnetocaloric effect and its relation to shape-memory properties in ferromagnetic Heusler alloys. *J. Phys. Condens. Matter* **2009**, *21*, 233201.
16. Khovaylo, V.V.; Oikawa, K.; Abe, T.; Tagaki, T. Entropy change at the martensitic transformation in ferromagnetic shape memory alloys Ni2+xMn1-xGa. *J. Appl. Phys.* **2003**, *93*, 8483–8485.
17. Barandiarán, J.M.; Chernenko, V.A.; Cesari, E.; Salas, D.; Gutiérrez, J.; Lázpita, P. Magnetic field and atomic order effect on the martensitic transformation of a metamagnetic alloy. *J. Phys. Condens. Matter* **2013**, *25*, 484005.
18. Recarte, V.; Pérez-Landazábal, J.I.; Sánchez-Alarcos, V. Dependence of the relative stability between austenite and martensite phases on the atomic order in a Ni-Mn-In Metamagnetic Shape Memory Alloy. *J. Alloy. Comp.* **2012**, *536*, S308–S311.
19. Recarte, V.; Pérez-Landazábal, J.I.; Sánchez-Alarcos, V.; Rodríguez-Velamazán, J.A. Dependence of the martensitic transformation and magnetic transition on the atomic order in Ni-Mn-In Metamagnetic Shape Memory Alloys. *Acta Mater.* **2012**, *60*, 1937–1945.
20. Sánchez-Alarcos, V.; Pérez-Landazábal, J.I.; Recarte, V.; Cuello, G.J. Correlation between atomic order and the characteristics of the structural and magnetic transformations in Ni-Mn-Ga shape memory alloys. *Acta Mater.* **2007**, *55*, 3883–3889.
21. Sánchez-Alarcos, V.; Pérez-Landazábal, J.I.; Recarte, V.; Rodríguez-Velamazán, J.A.; Chernenko, V.A. Effect of atomic order on the martensitic and magnetic transformations in Ni-Mn-Ga ferromagnetic shape memory alloys. *J. Phys. Condens. Matter* **2010**, *22*, 166001.
22. Sánchez-Alarcos, V.; Pérez-Landazábal, J.I.; Recarte, V.; Lucia, I.; Vélez, J.; Rodríguez-Velamazán, J.A. Effect of high temperature quenching on the magnetostructural transformations and the

long-range atomic order of Ni-Mn-Sn and Ni-Mn-Sb metamagnetic shape memory alloys. *Acta Mater.* **2013**, *61*, 4676–4682.

23. Ito, W.; Imano, Y.; Kainuma, R.; Sutou, Y.; Oikawa, K.; Ishida, K. Martensitic and magnetic transformation behaviors in Heusler-type NiMnIn and NiCoMnIn metamagnetic shape memory alloys. *Metall. Mater. Trans.* **2007**, *38*, 759–766.
24. Pérez-Landazábal, J.I.; Recarte, V.; Sánchez-Alarcos, V.; Gómez-Polo, C.; Cesari, E. Magnetic properties of the martensitic phase in Ni-Mn-In-Co metamagnetic shape memory alloys. *Appl. Phys. Lett.* **2013**, *102*, 101908.
25. Kainuma, R.; Imano, Y.; Ito, W.; Sutou, Y.; Morito, H.; Okamoto, S.; Kitakami, O.; Kanomata, T.; Ishida, K. Magnetic-field-induced shape recovery by reverse phase transformation. *Nature* **2006**, *439*, 957–960.
26. Kustov, S.; Corró, M.L.; Pons, J.; Cesari, E. Entropy change and effect of magnetic field on martensitic transformation in a metamagnetic Ni-Co-Mn-In shape memory alloy. *Appl. Phys. Lett.* **2009**, *94*, 191901.
27. Santamarta, R.; Cesari, E.; Font, J.; Muntasell, J.; Pons, J.; Dutkiewicz, J. Effect of atomic order on the martensitic transformation of Ni-Fe-Ga alloys. *Scripta Mater.* **2006**, *54*, 1985–1989.
28. Planes, A.; Mañosa, Ll.; Vives, E.; Rodriguez-Carvajal, J.; Morin, M.; Guenin, G. Neutron diffraction study of long-range atomic order in Cu-Zn-Al shape memory alloys. *J. Phys. Condens. Matter* **1992**, *4*, 553.
29. Essam, J.W.; Fisher, M.E. Padé approximant studies of the lattice gas and ising ferromagnet below the critical point. *J. Chem. Phys.* **1963**, *38*, 802.
30. Miyamoto, T.; Ito, W.; Umetsu, R.Y.; Kainuma, R.; Kanomata, T.; Ishida, K. Phase stability and magnetic properties of $Ni_{50}Mn5_{0-x}In_x$ Heusler-type alloys. *Scripta Mater.* **2010**, *62*, 151–154.
31. Sánchez-Alarcos, V.; Recarte, V.; Pérez-Landazábal, J.I.; Gómez-Polo, C.; Rodríguez-Velamazán, J.A. Role of magnetism on the martensitic transformation in Ni-Mn-based magnetic shape memory alloys. *Acta Mater.* **2012**, *60*, 459–468.
32. Planes, A.; Mañosa, L. Vibrational properties of shape-memory alloys. *Solid State Phys.* **2001**, *55*, 159–267.
33. Recarte, V.; Pérez-Landazábal, J.I.; Kustov, S.; Cesari, E. Entropy change linked to the magnetic field induced martensitic transformation in a Ni-Mn-In-Co shape memory alloy. *J. Appl. Phys.* **2010**, *107*, 053501.
34. Recarte, V.; Pérez-Landazábal, J.I.; Sánchez-Alarcos, V.; Zablotskii, V.; Cesari, E.; Kustov, S. Entropy change linked to the martensitic transformation in metamagnetic shape memory alloys. *Acta Mater.* **2012**, *60*, 3168–3175.
35. Oikawa, K.; Omori, T.; Sutou, Y.; Morito, H.; Kainuma, R.; Ishida, K. Phase equilibria and phase transition of the Ni-Fe-Ga ferromagnetic shape memory alloy system. *Metall. Mater. Trans.* **2007**, *338*, 767–776.